The Simulation of the Two-Dimensional Ising Model on the Creutz Cellular Automaton for the Fractals Obtained by Using the Model of Diffusion-Limited Aggregation

Ziya Merdan[a], Mehmet Bayirli[b], and Mustafa Kemal Ozturk[c]

[a] Faculty of Arts and Sciences, Department of Physics, Kirikkale University, Kirikkale, Turkey
[b] Faculty of Arts and Sciences, Department of Physics, Balikesir University, Balikesir, Turkey
[c] Department of Mineral Analysis and Teknology, MTA, Ankara, Turkey

Reprint requests to Z. M.; E-mail: zmerdan1967@hotmail.com

The fractals are obtained by using the model of diffusion-limited aggregation (DLA) for the lattice with L = 80, 120, and 160. The values of the fractal dimensions are compared with the results of former studies. As increasing the linear dimensions they are in good agreement with those. The fractals obtained by using the model of DLA are simulated on the Creutz cellular automaton by using a two-bit demon. The values computed for the critical temperature and the static critical exponents within the framework of the finite-size scaling theory are in agreement with the results of other simulations and theoretical values.

Key words: Ising Model; Finite-Size Scaling; Cellular Automaton; Fractals.
PACS numbers: 05.50.+q, 64.60. Cn, 75.40. Cx, 75.40.Mg

1. Introduction

The diffusion-limited aggregation (DLA) model was first introduced in 1981 by Witten and Sander [1, 2]. The application of fractal concepts, which were first introduced by Mandelbrot et al. to describe complex natural shapes and structures as well as mathematical sets and functions having an intricately irregular form, has been studied [3 – 6]. The aggregation of particles to form cluster has, for a long time, been one of the central phenomena in natural science with important implications for physical problems such as air pollution, dielectric breakdown, bacterial colony growth, and natural formations (e. g. snowflakes and manganese dendrites). The model allowing exploration of the process of pattern formation in real physical systems is based mostly on the model of diffusion-limited aggregation. This model describes the most important morphology patterns observed in various non-equilibrium systems, such as DLA-like, dendrite, needle, treelike, dense-branching, compact, stingy, spiral, and chiral structures [7 – 14]. In this paper, we obtained fractals by using the model of DLA for the lattice with L = 80, 120, and 160. The fractal dimensions obtained for the fractal clusters were also compared with results of other studies [15 – 21].

The Creutz cellular automaton [22] has simulated the two-dimensional Ising model successfully near the critical region, and has reproduced its critical exponents within the framework of the finite-size scaling theory [23, 24]. This algorithm is an order of magnitude faster than the conventional Monte Carlo method and does not need high quality random numbers. These features of the Creutz cellular automaton would make the Ising model simulations in higher dimensions more practical. Compared to the Q2R cellular automaton – that is a two-state-per-site cellular automaton which is both deterministic and reversible (see [25] for details) – it has the advantage of allowing the specific heat to be computed from the internal energy fluctuations. In the present work, the fractals obtained by using the model of DLA are first simulated on the Creutz cellular automaton by using a two-bit demon. The purpose of this paper is to test the finite-size scaling relations for the Ising model in $d = 2$ dimensions. The simulations are carried out on the Creutz cellular automaton, which has successfully arisen as an alternative research tool for Ising models in the dimensionalities $2 \leq d \leq 8$ [26].

The model is introduced in Section 2, the results are discussed in Section 3, and a conclusion is given in Section 4.

2. Model

In the model of DLA, the initial state is a seed particle at the origin of a lattice. A second particle is added at some random site at large distance from the origin. This particle walks randomly until it visits a site adjacent to the seed. Then the walking particle becomes part of the cluster. Another particle is now introduced at a random distant point, and so on. If a particle touches the boundaries of the lattice in its random walk it is removed and another one is introduced. The fractals in Figure 1 have been obtained by using the model of DLA for the lattice with L = 80, 120, and 160.

The two-dimensional Ising model for the fractal obtained by using the model of DLA at Figure 1 is simulated on the Creutz cellular automaton. In the Creutz cellular automaton, four binary bits are associated with each site of the lattice. The value for each site is determined from its value and those of its nearest neighbours at the previous time step. The updating rule, which defines a deterministic cellular automaton, is as follows. Of the four binary bits on each site, the first
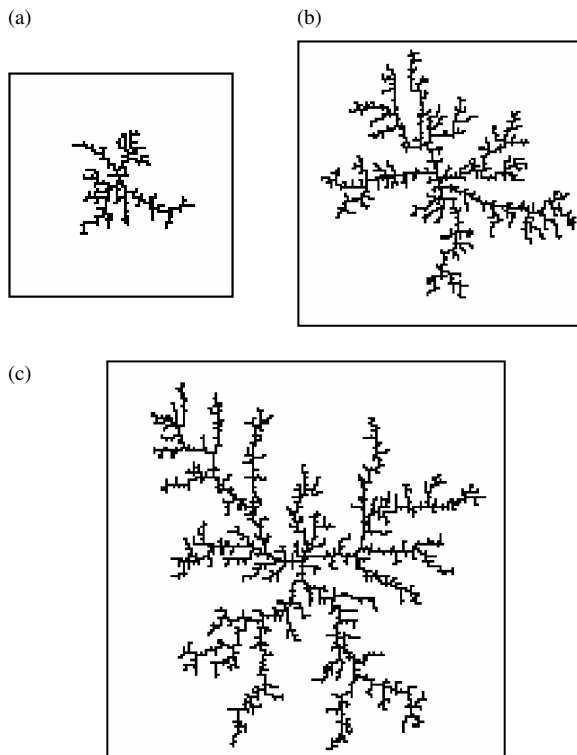
(a)

(b)

(c)

Fig. 1. Images of the fractals obtained by using the model of DLA for lattices with the linear dimensions (a) L = 80, (b) L = 120, and (c) L = 160.

one is the Ising spin B_i. Its value may be '0' or '1'. The Ising spin energy (internal energy) of the lattice, H_I, is given (in units of the nearest neighbour coupling constant J) by

$$H_I = -J \sum_{\langle i,j \rangle} S_i S_j, \qquad (1)$$

where $S_i = 2B_i - 1$, and $\langle i, j \rangle$ denotes the sum over all nearest neighbour pairs of sites. The second and the third bits are for the momentum variable conjugate to the spin (the demon). These two bits form an integer which can take on the value 0, 1, 2, or 3. The kinetic energy (in units of J) associated with the demon can take on four times these integer values. The total energy

$$H = H_I + H_K \qquad (2)$$

is conserved; here H_K is the kinetic energy of the lattice. For a given total energy the system temperature T (in units of J/k_B, where k_B is the Boltzmann constant) is obtained from the average value of the kinetic energy. The fourth bit provides a checkerboard style updating, and so it allows the simulation of the Ising model on a cellular automaton. The black sites of the checkerboard are updated and then their colour is changed into white: the white sites are changed into black without being updated.

The updating rules for the spin and the momentum variables are as follows: For a site to be updated its spin is flipped and the change in the Ising energy (internal energy) H_I is calculated. If this energy change is transferable to or from the momentum variable associated with this site, such that the total energy H is conserved, then this change is done and the momentum is appropriately changed. Otherwise the spin and the momentum are not changed.

As the initial configuration all spins are taken ordered (up or down). The initial kinetic energy is given to the lattice via the second bits of the momentum variables in the white sites randomly. The quantities computed are averages over the lattice and the number of time steps during which the cellular automaton develops.

The simulations are carried out on simple hypercubic lattices L^2 of linear dimensions $80 \leq L \leq 160$ with periodic boundary conditions by using two-bit demons. The cellular automaton develops 9.6×10^5 (L = 80, 120, 160) sweeps for each run with 7 runs for each total energy.
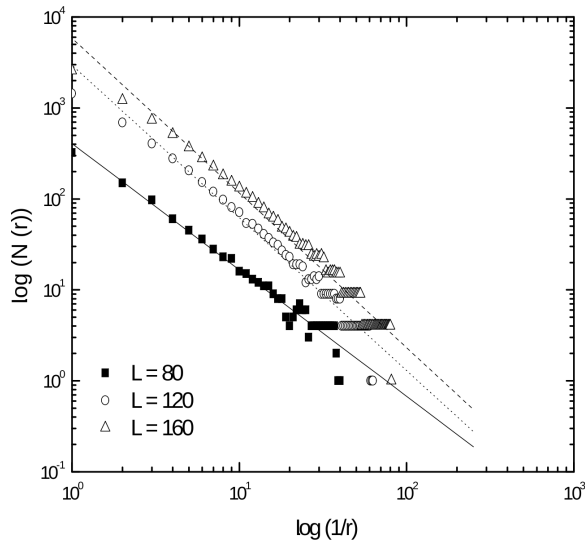
Fig. 2. The log-log plot of $N(r)$ versus $1/r$ with the slopes giving the values of $D = 1.389(52)$ (■) (Fit interval $1-40$), $D = 1.678(43)$ (○) (Fit interval $1-63$), and $D = 1.701(32)$ (▲) (Fit interval $1-81$) for the lattice with L = 80, 120, and 160, respectively.

3. Results and Discussion

The fractals obtained by using the model of diffusion-limited aggregation are illustrated in Figure 1 for the lattice with L = 80, 120, and 160.

We used the mass-radius method to determine the fractal dimensions of Figure 1. The mass-radius method [7, 9] is based on finding the relation between the mass $N(r)$, within circles of radius r whose origin is placed at a point on the object, i. e. the distance r. The fractal dimension is then determined from the relation

$$N(r) \propto (1/r)^{-D}. \tag{3}$$

In order to apply this method, we assumed that $N(r)$ is proportional to the length of the traced branch within a circle of radius r. The fractal dimension D was obtained from the slope of the log-log plots of $N(r)$ versus $1/r$, and the standard error was calculated using a linear regression method. We verified the accuracy of this procedure by analysing a mathematical Hausdorff set known as a Koch curve with $D = \log 3 / \log 2$. The log-log plots of $N(r)$ against $1/r$ are illustrated in Figure 2 for the lattice with L = 80, 120, and 160.

The computed values of $D = 1.389(52)$, $D = 1.678(43)$, and $D = 1.701(32)$ whose fit intervals are $1-40$, $1-63$, $1-81$, respectively, are in agreement
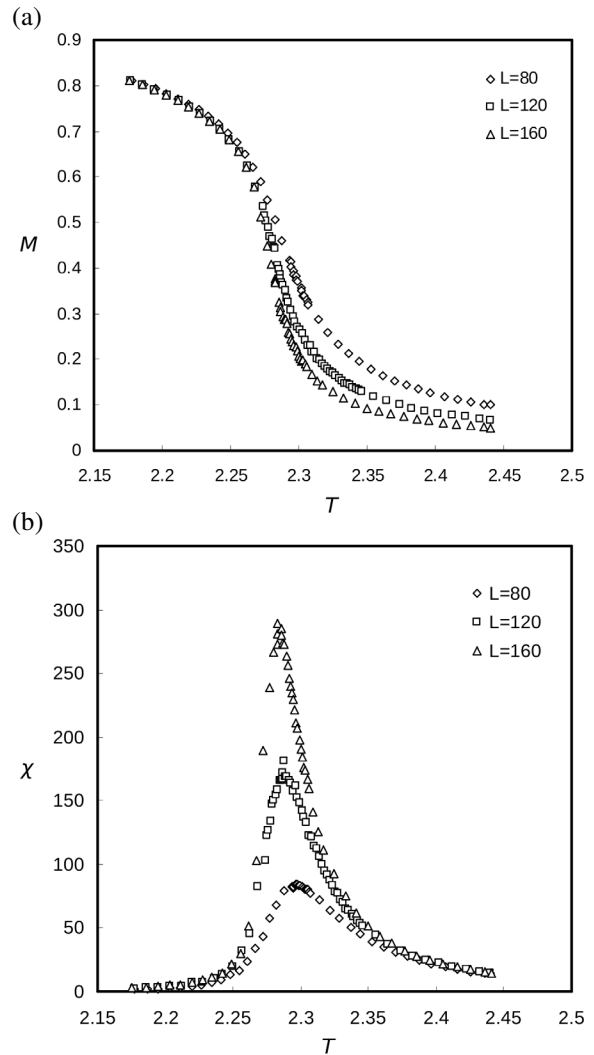

Fig. 3. Temperature dependence of (a) the order parameter (M) and (b) the magnetic suscebtibility (χ) of the two-dimensional Ising model for the lattice with L = 80, 120, and 160.

with $D = 1.8753(6)$, $D = 1.8752(8)$, $D = 1.9476(3)$, $D = 1.9473(4)$ whose fit intervals are $64-512$, and $D = 1.665(3)$ whose fit interval is $8-48$ [15], $D = \frac{187}{96} = 1.9479\ldots$ (the exact prediction) [16], $D = \frac{5}{3} = 1.666\ldots$ [17], $D = 1.87(1)$ [18], $D = \frac{15}{8} = 1.875$ (the exact prediction) [19], $D = \frac{11}{8}$ (the exact prediction) [20, 21].

In $d = 2$ dimensions, the finite-size scaling theory gives the following scaling forms for the quantities of interest [23, 24, 27]:
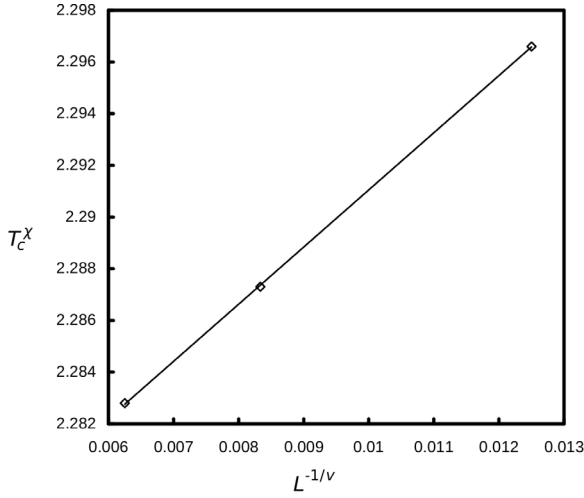
$$M = L^{-\beta/\nu} X(x), \tag{4}$$

Fig. 4. Value of the infinite-lattice critical temperature for the magnetic susceptibility χ_{max}; $T_c^\chi = 2.2689$ was obtained by extrapolating the straight line fitted to the critical temperature of the lattice with the linear dimension $80 \leq L \leq 160$.
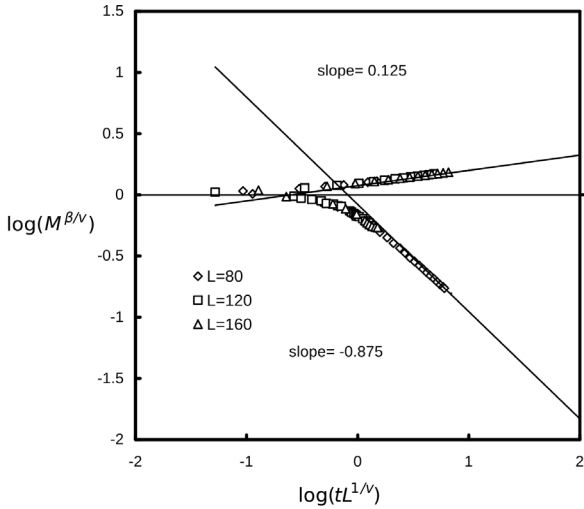

Fig. 5. Finite-size scaling plot for the order parameter M for $T < T_c(\infty)$ ($\beta = 0.125$) and for $T > T_c(\infty)$ ($\beta' = 0.875$); $t = |T - T_c(\infty)|/T_c(\infty)$.

$$\chi = L^{\gamma/\nu} Y(x), \tag{5}$$

where $x = tL^{1/\nu}$, $t = |T - T_c|/T_c$ is the reduced temperature, and T_c is the critical temperature of the infinite lattice. The shape functions X and Y behave asymtotically as

$$X(x) = Bx^\beta, \tag{6}$$

$$Y(x) = Gx^{-\gamma}. \tag{7}$$

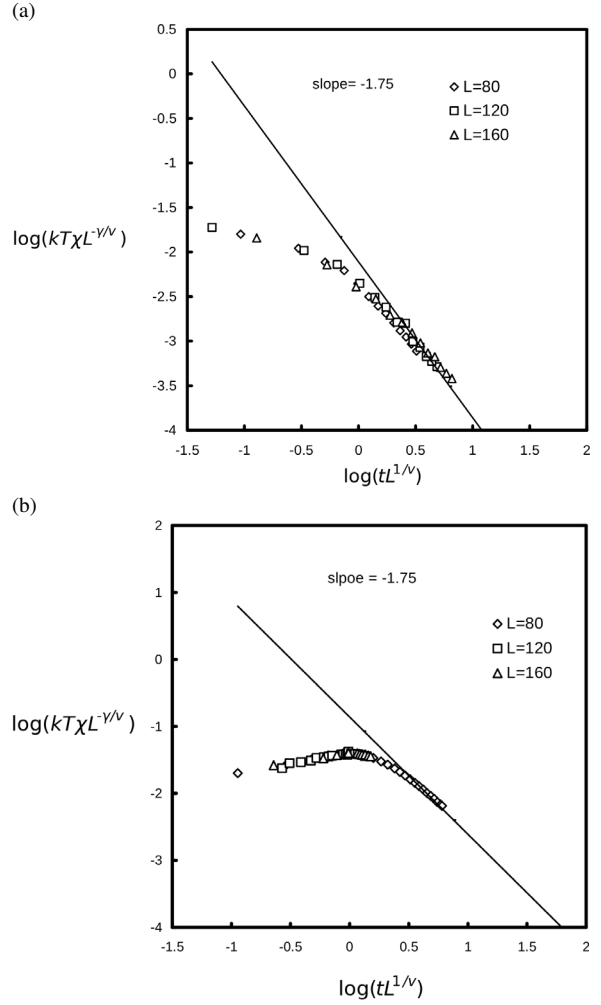Fig. 6. Finite-size scaling plot for the susceptibility χ. (a) $T < T_c(\infty)$, $t = |T - T_c(\infty)|/T_c(\infty)$; (b) $T > T_c(\infty)$, $t = |T - T_c(\infty)|/T_c(\infty)$.

(4) and (5) take the following forms at $T = T_c$:

$$M \propto L^{-\beta/\nu}, \tag{8}$$

$$\chi \propto L^{\gamma/\nu}, \tag{9}$$

and at $T = T_c(L)$,

$$\chi_{max} \propto L^{\gamma/\nu}. \tag{10}$$

The finite-size scaling relation for $T_c(L)$ is

$$T_c - T_c(L) \propto L^{-1/\nu}. \tag{11}$$

The critical exponents α, β, γ, and ν are those of the infinite lattice. Since $\nu = 1$ in $d = 2$ dimensions,
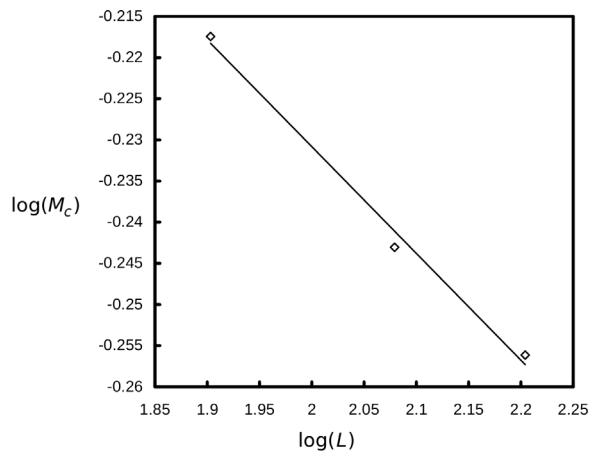
Fig. 7. The log-log plot of M_c against L ($80 \leq L \leq 160$) with the slope giving the value of $\beta/v = 0.1297$.

(11) takes the following form:

$$T_c - T_c(L) \propto L^{-1}. \tag{12}$$

The temperature dependence of the order parameter M and the magnetic susceptibility χ are illustrated in Figure 3.

The maxima for the magnetic susceptibility occurs at $T_c^\chi(80) = 2.2966$, $T_c^\chi(120) = 2.2873$, and $T_c^\chi(160) = 2.2828$, respectively. (12) is used to get the critical temperature of the infinite lattice (Fig. 4).

The computed value of $T_c = 2.2689$ is in better agreement with the theoretical prediction of $T_c(\infty) = 2.269$ [23, 24, 27] and the Creutz cellular automaton $T_c(\infty) = 2.263$ [24].

The data obtained for the order parameter M were analyzed by using the finite-size scaling plot given in Figure 5.

The data lie on a single curve for temperatures both above and below $T_c = 2.2689$, and validate the finite-size scaling. The straight line passing through the data for $T < T_c(\infty)$ in Figure 5 describes (6). The straight line passing through the data for $T > T_c(\infty)$ behaves according to this equation with $\beta' = 1 - \beta$ replacing β and some other constant replacing B. Thus, the data for M are in agreement with the theoretical value $\beta = 0.125$ for $T < T_c(\infty)$ and $\beta' = 0.875$ for $T > T_c(\infty)$.

The data obtained for the susceptibility χ were analyzed by making use of the finite-size scaling plot given in Figure 6.

The data lie on a single curve for temperatures both above and below $T_c = 2.2689$, and validate the finite-size scaling. The straight line passing through the data
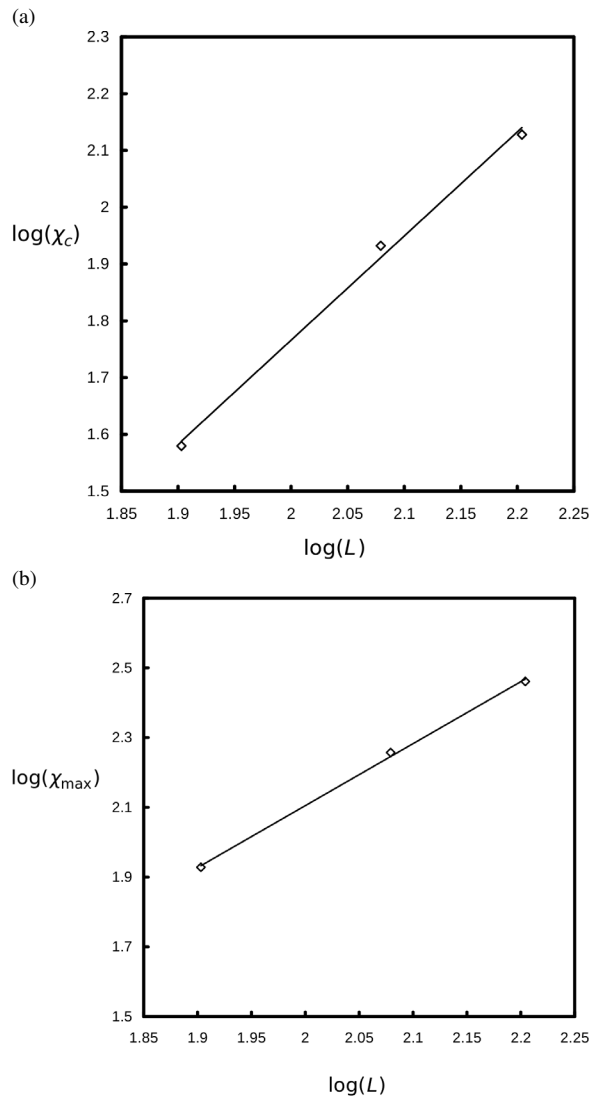

Fig. 8. (a) log-log plot of χ_c against L ($80 \leq L \leq 160$) with the slope giving the value of $\gamma/v = 1.8333$; (b) log-log plot of $\chi_{\max}$ against L ($80 \leq L \leq 160$) with the slope giving the value of $\gamma/v = 1.777$.

for $T < T_c(\infty)$ and $T > T_c(\infty)$ in Figure 6 describes (7). The scaling of the susceptibility data agrees well with the asymtotic form, and with the critical exponent $\gamma = 1.75$ for $T > T_c(\infty)$ and $T < T_c(\infty)$.

The slope of the log-log plot of $M_c(L)$ against L in Figure 7, described by (8), gives the result of $\beta/v = 0.1297$ at $T_c = 2.2689$, which is in good agreement with the theoretical value $\beta/v = 0.125$.

The slope of the log-log plot of $\chi_c(L)$ against L in Figure 8a, described by (9), gives the result of $\gamma/v =$

1.8333 at $T_c = 2.2689$, which is in agreement with the theoretical value $\gamma/v = 1.75$. The slope of the log-log plot of $\chi_{\max}(L)$ against L in Figure 8b, described by (10), gives the result of $\gamma/v = 1.777$ at $T = T_c(L)$. It is in agreement with the theoretical value $\gamma/v = 1.75$, and reveals that the finite-size scaling relation for $\chi(L)$ at $T = T_c(L)$ is also valid at $T = T_c^{\chi}(L)$.

4. Conclusion

In this study, we obtained the fractals by using the model of DLA for the lattice with L = 80, 120, and 160. The fractal dimensions have been obtained for the fractal clusters. The fractal dimension is consistent with the results of other works as the linear dimension increases. The two-dimensional Ising model for the fractals obtained by using the model of DLA is simulated on the Creutz cellular automaton using the finite-size lattices with the linear dimension L = 80, 120, and 160. By the analysis of data within the framework of the finite-size scaling theory the critical temperature and the static critical exponents for the order parameter and the susceptibility are obtained. They are in agreement with the results of the Creutz cellular automaton and theoretical values within the error limits.

The computer used was an Intel(R) Core(TM)2 Duo CPU E6550 at 2.33 GHz. The CPU time invested was 980 h for all the simulations.

[1] T. A. Witten and L. M. Sander, Phys. Rev. Lett. **47**, 1400 (1980).
[2] T. A. Witten and L. M. Sander, Phys. Rev. B. **27**, 5686 (1983).
[3] T. Vicsek, Fractal Growth Phenomena, Word Scientific, Singapore 1989.
[4] B. B. Mandelbrot and M. Frame, Fractals, Encyclopedia of Physical Science and Technology, Academic, San Francisco 1982.
[5] B. B. Mandelbrot, An Introduction to Multifractal Distribution Functions, in Random Fluctuations and Pattern Growth: Experiment and Models Eds. H. E. Stanley and N. Ostrowsky, Kluwer, Dordrecht 1988.
[6] Z. Merdan and M. Bayirli, Chin. Phys. Lett. **22**, 2112 (2005).
[7] S. R. Forrest and T. A.Witten, J. Phys. A: Math. Gen. **12**, L109 (1979).
[8] F. Family, B. R. Masters, and D. Platt, Physica D **38**, 98 (1989).
[9] L. Niemeyer, L. Pietrenero, and H. J. Wiesmann, Phys. Rev. Lett. **52**, 1033 (1984).
[10] M. Matsushita, M. Sano, H. Hanjo, and Y. Savada, Phys. Rev. Lett. **53**, 286 (1984).
[11] H. Fijikawa and M. Matsushita, J. Phys. Soc. Japan **58**, 3875 (1989).
[12] S.-Y. Huang, X.-W. Zou, Z.-J. Tan, and Z.-Z. Jin, Phys. Lett. A **292**, 141 (2001).
[13] Z.-J. Tan, X.-W. Huang Zou, and Z.-Z. Jin, Phys. Lett. A **282**, 121 (2001).
[14] M. Lattuada, H. Wu, and M. Mordibelli, J. Coll. Int. Sci. **268**, R106 (2003).
[15] W. Janke and A. M. J. Schakel, Phys. Rev. E **71**, 036703 (2005).
[16] A. L. Stella and C. Vanderzande, Phys. Rev. Lett. **62**, 1067 (1989).
[17] H. Saleur and B. Duplantier, Phys. Rev. Lett. **58**, 2325 (1987).
[18] J. Asikainen, A. Aharony, B. B. Mandelbrot, E. M. Rauch, and J.-P. Hovi, Eur. Phys. J. B **34**, 479 (2003).
[19] H. E. Stanley, J. Phys. A 10, **L211** (1977).
[20] C. Vanderzande and A. L. Stella, J. Phys. A **22**, L445 (1989).
[21] B. Duplantier, Phys. Rev. Lett. **84**, 1363 (2000).
[22] M. Creutz, Ann. Phys. **167**, 62 (1986).
[23] V. Privman (Ed.), Finite Size Scaling and Numerical Simulation of Statistical Systems, Word Scientific, Singapore, 1990.
[24] B. Kutlu and N. Aktekin, J. Stat. Phys. **75**, 757 (1994); B. Kutlu and N. Aktekin, Physica A **208**, 423 (1994); B. Kutlu and N. Aktekin, Physica A **215**, 370 (1995).
[25] G. Y. Vichniac, Physica D **10**, 96 (1984); Y. Pomeau, J. Phys. A **17**, L145 (1984); H. J. Hermann, J. Stat. Phys. **45**, 145 (1986); W. M. Lang and D. Stauffer, J. Phys. A **20**, 5413 (1987).
[26] Z. Merdan, B. Boyacıoğlu, A. Günen, and Z. Sağlam, Bull. Pur. Appl. Scienc. D **22**, 95 (2003); Z. Merdan, A. Günen, and G. Mülazımoğlu, Int. J. Mod. Phys. C **16**, 1269 (2005); Z. Merdan, A. Günen, and Ş. Çavdar, Physica A **359**, 415 (2006); Z. Merdan and R. Erdem, Phys. Lett. A **330**, 403 (2004); Z. Merdan and M. Bayırlı, Appl. Math. Comp. **167**, 212 (2005); Z. Merdan, A. Duran, D. Atille, G. Mülazımoğlu, and A. Günen, Physica A **366**, 265 (2006); Z. Merdan and D. Atille, Physica A **376**, 327 (2007); Z. Merdan and D. Atille, Mod. Phys. Lett. B **21**, 215 (2007); G. Mülazimoglu, A. Duran, Z. Merdan, and A. Günen, Mod. Phys. Lett. B **13**, 1329 (2008); Z. Merdan, M. Bayirli, and M. K. Oztürk, Z. Naturforsch. **64a**, 849 (2009).
[27] N. Aktekin, in: Annual Reviews of Computational Physics, Vol. VII, (Ed.: D. Stauffer), Word Scientific, Singapore 2000, p. 1.